Journal of Clinical Neuroscience xxx (xxxx) xxx

Contents lists available at ScienceDirect

Journal of Clinical Neuroscience

journal homepage: www.elsevier.com/locate/jocn

Clinical study

Differentiating between glioblastomas with and without isocitrate dehydrogenase gene mutation by findings on conventional magnetic resonance images

Tetsuya Shimizu [a,*], Satoshi Matsushima [a], Nei Fukasawa [b], Yasuharu Akasaki [c], Ryosuke Mori [c], Hiroya Ojiri [a]

[a] Department of Radiology, The Jikei University School of Medicine, Tokyo, Japan
[b] Department of Pathology, The Jikei University School of Medicine, Tokyo, Japan
[c] Department of Neurosurgery, The Jikei University School of Medicine, Tokyo, Japan

ARTICLE INFO

Article history:
Received 4 February 2020
Accepted 5 April 2020
Available online xxxx

Keywords:
Glioblastoma
Isocitrate dehydrogenase
Magnetic resonance imaging
Diagnostic imaging

ABSTRACT

Various studies using advanced techniques have estimated the isocitrate dehydrogenase (IDH) gene mutation status in glioblastoma (GBM) from preoperative images. However, it is important to be able to predict mutation status using conventional MRI, which is more widely used in clinical practice. In this study, we examined the features of GBM with and without IDH gene mutation on conventional MRI. Twenty-three patients with GBM in whom IDH gene mutation status had been pathologically and molecularly confirmed in tumor specimens were included. The cases were divided into an IDH-wildtype group (n = 17) and an IDH-mutant group (n = 6). We retrospectively compared the following imaging parameters between the two groups: tumor location (superficial or deep), borders on T2-weighted images (regular or irregular), borders of enhancing lesions (regular or irregular), number of lesions showing contrast enhancement (solitary or multiple), presence or absence of intralesional bleeding, and presence or absence of a low-grade glioma in the background around the enhancing lesion. IDH-wildtype tumors were significantly more likely to be superficial than were IDH-mutant tumors ($p < 0.05$). Enhancing lesions in the IDH-wildtype group were less likely to have an irregular border ($p = 0.059$). Low-grade glioma was a background lesion in 5 patients (83.3%) in the IDH-mutant group and 9 (52.9%) in the IDH-wildtype group. The IDH mutation status is likely to be wildtype in patients with superficial GBM in which the enhancing lesion has a regular border and when low-grade glioma is not found as a background lesion on MRI.

1. Introduction

Brain tumors have traditionally been classified by histogenesis, including the microscopic similarities of cells presumed to be of tumor origin and their presumed degree of differentiation. However, molecular classification is now possible and is included in the revised 2016 World Health Organization Classification of Tumors of the Central Nervous System [1].

Glioblastoma (GBM) is now broadly classified according to isocitrate dehydrogenase (IDH) gene mutation status in the 2016 World Health Organization (WHO) classification. GBM is divided into glioblastoma, IDH-wildtype (IDH-wildtype GBM); glioblastoma, IDH-mutant (IDH-mutant GBM); and glioblastoma, NOS, which is a diagnosis reserved for tumors for which full IDH evaluation cannot be performed [1].

Most cases of IDH-wildtype GBM are thought to be primary or de novo without a background lesion and most cases of IDH-mutant GBM are considered to develop secondary to a lower-grade glioma [1,2]. It has been reported that IDH-mutant GBM occurs in younger patients and has a better prognosis than IDH-wildtype GBM [1,2].

Various studies using advanced techniques and methods have attempted to predict IDH gene mutation status from preoperative images; however, in daily practice, prediction with conventional MRI, which is widely used clinically, is more important but remains a challenging task. In this study, we examined the imaging features of GBM according to IDH gene mutation status using conventional MRI images.

* Corresponding author at: Department of Radiology, The Jikei University School of Medicine, 3-25-8, Nishi-Shimbashi, Minato-ku, Tokyo 105-8461, Japan.
E-mail address: tshimizu@jikei.ac.jp (T. Shimizu).

https://doi.org/10.1016/j.jocn.2020.04.016
0967-5868/

2. Material and methods

2.1. Subjects

Twenty-three patients with a diagnosis of GBM who underwent surgery at our hospital between January 1, 2013 and August 31, 2017 and whose IDH gene mutation status was determined pathologically and molecularly using tumor specimens were retrospectively identified and enrolled in the study. The 23 patients comprised 13 men and 10 women of mean age 56.7 (range 30–81) years. We searched for both IDH-1 and IDH-2 gene mutations and identified tumors without either mutation as IDH-wildtype GBM. IDH-wildtype GBM was identified in 17 cases (11 men, 6 women; mean age 58.6 [range 30–81] years) and IDH-mutant GBM in 6 (2 men, 4 women; mean age 51.3 [range 42–62] years). All IDH-mutant GBM had a genetic mutation of IDH-1. Four of the 17 patients with IDH-wildtype GBM had undergone surgery for their disease before the study period and underwent repeat surgery for recurrent lesions; 3 of these four patients had also received chemoradiotherapy at the time of their previous surgery. The pathological histology at the time of surgery was GBM in 2 of the 4 cases, anaplastic astrocytoma in 1, and diffuse astrocytoma in 1. Furthermore, 3 of 6 cases of IDH-mutant GBM underwent repeat surgery for a recurrent lesion, and all had received chemoradiotherapy; 1 of these patients received neoadjuvant therapy, including bevacizumab, just before undergoing MRI. The pathological histology at the time of previous surgery was GBM in 1 case and anaplastic astrocytoma in 2 cases.

The most recent preoperative MRI scans were used for evaluation and the images acquired before the earliest operation during the study period were used for patients in whom multiple operations had been performed. When the first operation was performed before the study period, the images at the time of the second and subsequent operations were used. MRI, including T2-weighted imaging (T2WI), fluid-attenuated inversion recovery (FLAIR) sequences, contrast-enhanced spin echo T1-weighted imaging (T1WI), and contrast-enhanced three-dimensional gradient recalled-echo T1WI, was performed in all cases, and susceptibility weighted imaging (SWI) was performed in all patients except for 2 who were excluded from evaluation of hemorrhage. The average interval between MRI and surgery was 12.9 (0–59) days. Table 1 shows each patient's age and sex and the interval between MRI and surgery. One patient with neurofibromatosis type 1 was excluded because of the expected influence of genes other than the IDH gene.

The study protocol was approved by the ethics committee of The Jikei University School of Medicine. All human studies were performed in accordance with the ethical standards of the institution and with the 1964 Helsinki declaration and its later amendments. Formal consent was not required for this type of study. This article does not contain any studies with animals performed by any of the authors.

Table 1
Patient age and sex and the interval between imaging and surgery.

	All patients (n = 23)	IDH-wildtype (n = 17)	IDH-mutant (n = 6)
Age, years			
Mean	56.7	58.6	51.3
Range	30–81	30–81	42–62
Sex			
Male	13	11	2
Female	10	6	4
Interval between examination and surgery, days			
Mean	12.9	14.1	9.5
Range	0–59	1–59	0–19

IDH, isocitrate dehydrogenase.

2.2. Imaging

MRI scans were acquired using 1.5-T or 3-T clinical scanners (Magnetom Avanto or Magnetom Skyra; Siemens, Erlangen, Germany). The protocol included the following sequences:

(1) T2WI-FS on 1.5 T (TR/TE, 3500/94 ms; flip angle, 180°; slice thickness, 5 mm; section gap, 1.5 mm; matrix, 256 × 256; FS, chemical shift selective; bandwidth, 119 Hz/Px; scan time, 1 min 54 s; field of view [FOV], 210 × 210 mm)
(2) T2WI-FS on 3 T (TR/TE, 4500/96 ms; flip angle, 150°; slice thickness, 4 mm; section gap, 1.4 mm; matrix, 314 × 448; FS, chemical shift selective; bandwidth, 196 Hz/Px; scan time, 1 min 17 s; FOV, 220 × 206 mm)
(3) FLAIR on 1.5 T (TR/TE, 9000/99 ms; TI, 2500 ms; flip angle, 150°; slice thickness, 5 mm; section gap, 1.5 mm; matrix, 230 × 256; bandwidth, 190 Hz/Px; scan time, 2 min 26 s; FOV, 210 × 210 mm)
(4) FLAIR on 3 T (TR/TE, 9000/102 ms; TI, 2500 ms; flip angle, 170°; slice thickness, 5 mm; section gap, 1.6 mm; matrix, 192 × 384; bandwidth, 255 Hz/Px; scan time, 1 min 48 s; FOV, 209 × 220 mm)
(5) SWI on 1.5 T (TR/TE, 49/40 ms; flip angle, 15°; slice thickness, 2 mm; section gap, 0 mm; matrix, 160 × 256; bandwidth, 80 Hz/Px; scan time, 2 min 05 s; FOV, 187.5 × 240 mm)
(6) SWI on 3 T (TR/TE, 28/20 ms; flip angle, 15°; slice thickness, 1.3 mm; section gap, 0 mm; matrix, 184 × 320; bandwidth, 120 Hz/Px; scan time, 2 min 01 s; FOV, 187.5 × 240 mm)
(7) Contrast-enhanced spin-echo T1WI on 1.5 T (TR/TE, 450/9.6 ms; flip angle, 130°; slice thickness, 5 mm; section gap, 1.5 mm; matrix, 230 × 256; bandwidth, 150 Hz/Px; scan time, 1 min 20 s; FOV, 210 × 210 mm)
(8) Contrast-enhanced spin-echo T1WI on 3 T (TR/TE, 450/7.9 ms; flip angle, 150°; slice thickness, 4 mm; section gap, 1.6 mm; matrix, 240 × 320; bandwidth, 504 Hz/Px; scan time, 2 min 12 s; FOV, 220 × 220 mm)
(9) Contrast-enhanced 3D gradient recalled-echo T1WI on 1.5 T (TR/TE, 7.08/3.33 ms; flip angle, 10°; slice thickness, 0.9 mm; section gap, 0 mm; matrix, 256 × 256; FS, Q-fat; bandwidth, 200 Hz/Px; scan time, 2 min 54 s; FOV, 230 × 187 mm)
(10) Contrast-enhanced 3D gradient recalled-echo T1WI on 3 T (TR/TE, 8.3/3.69 ms; flip angle, 9°; slice thickness, 0.9 mm; section gap, 0 mm; matrix, 320 × 272; FS, Q-fat; bandwidth, 210 Hz/Px; scan time, 2 min 54 s; FOV, 220 × 195 mm); sagittal and coronal images were obtained by multiplanar reconstruction based on the original images of the transverse images acquired.

2.3. Evaluation of images

The differences between the images obtained in the IDH-wildtype GBM group were retrospectively compared with those obtained in the IDH-mutant GBM group. The examination parameters were the location of the lesion (superficial or deep), condition of the border on T2WI (regular or irregular), condition of the border of the enhancing lesion (regular or irregular), number of lesions showing contrast enhancement (solitary or multiple), intralesional bleeding status, and the presence or absence of a low-grade glioma around the enhancing lesion.

A lesion in which the enhancing component was in contact with the surface of the brain was deemed to be superficial and one in contact with the ventricle was considered deep. When the lesion

Please cite this article as: T. Shimizu, S. Matsushima, N. Fukasawa et al., Differentiating between glioblastomas with and without isocitrate dehydrogenase gene mutation by findings on conventional magnetic resonance images, Journal of Clinical Neuroscience, https://doi.org/10.1016/j.jocn.2020.04.016

was in contact with both the brain surface and ventricle, a lesion that was more in contact with the brain surface than the ventricle was taken as superficial and a lesion that was more in contact with the ventricle than the brain surface was taken as deep. Hemorrhagic status was evaluated based on the presence or absence of a low signal area on SWI; cases with no SWI scans available were not evaluated. Regardless of whether or not a low-grade glioma was detected in the background, we defined background low-grade glioma as "an infiltrative T2 prolongation area without contrast enhancement and with mild lower signal than edema, spreading further out of T2 prolongation area including edema around the enhancing lesion" and evaluated its presence or absence visually. When there were multiple lesions showing contrast enhancement, the largest one was evaluated. Images for both contrast-enhanced spin-echo T1WI and contrast-enhanced 3D gradient recalled-echo T1WI were used to evaluate lesions with contrast enhancement.

The examinations were performed by two neuroradiologists working independently, and any disagreements were resolved by consensus. Interobserver agreement was evaluated by calculating the weighted κ value.

2.4. Statistical analysis

Each of the 6 imaging parameters (location, condition of the border on T2WI, condition of the border of the enhancing lesion, number of lesions showing contrast enhancement, the presence or absence of bleeding in the lesion, and the presence or absence of a background low-grade glioma) was compared between patients with IDH-wildtype GBM and those with IDH-mutant GBM using Fisher's exact test. Interobserver agreement for each parameter was assessed by calculation of the weighted κ statistic. A value of 0–0.20 indicated slight agreement, 0.21–0.40 indicated fair agreement, 0.41–0.60 indicated moderate agreement, 0.61–0.80 suggested good agreement, and 0.81–1.00 meant very good agreement. The statistical analyses were performed using Bell Curve for Excel (version 2.14, Social Survey Research Information Co, Ltd, Tokyo, Japan). P-values <0.05 were considered statistically significant.

3. Results

A superficial tumor location was more common in the IDH-wildtype GBM group than in the IDH-mutant GBM group (70.6% [n = 12] vs 16.7% [n = 1]; p = 0.035) (Fig. 1). No significant difference was found in any of the other parameters; however, enhancing lesions were less likely to have an irregular border in the IDH-wildtype GBM group than in the IDH-mutant GBM group (35.3% [n = 6] vs 83.3% [n = 5]; p = 0.059) (Fig. 1). Background low-grade glioma was found in 5 cases (83.3%) in the IDH-mutant GBM group and in 9 cases (52.9%) in the IDH-wildtype GBM group (Figs. 2, 3). Table 2 shows the results for each imaging parameter evaluated.

3.1. Inter-rater reproducibility

There was very good interobserver agreement regarding superficial location (κ = 0.91, p < 0.001), an irregular border on T2WI (κ = 1, p < 0.001), irregular border enhancement (κ = 1, p < 0.001), multifocality (κ = 1, p < 0.001), hemorrhage (κ = 1, p < 0.001), and background low-grade glioma (κ = 0.91, p < 0.001).

4. Discussion

Various studies have attempted to predict IDH gene mutation status on preoperative images by estimating the presence/proportion of non-contrast-enhanced tumor tissue, location of the tumor, presence of cysts and satellites [3,4], tumor blood flow and areas of necrosis using arterial spin labeling [5], and detection of 2-hydroxyglutarate on MR spectroscopy [6]. There have also been reports of estimation using deep learning [7]. Some of these reports indicate that IDH gene mutations can be estimated from images with relatively high sensitivity but the findings are inconsistent and predictions using conventional MRI remain challenging. However, in daily practice, prediction with conventional MRI, which is widely used clinically, is most important. Therefore, in this study, we investigated if there were any findings on conventional MRI images that could predict IDH gene mutation status in patients with GBM.

The only statistically significant between-group difference on imaging was the location of the tumor, i.e., the GBM was superficial in a significantly greater number of patients in the IDH-wildtype group than in the IDH-mutant group. Moreover, the percentage of tumors with irregular border enhancement tended to be lower in the IDH-wildtype group. These findings suggest that GBM is more likely to be IDH-wildtype when an enhancing lesion is superficial and has a regular border. To the best of our knowledge, these results have not been reported before. Although these findings are

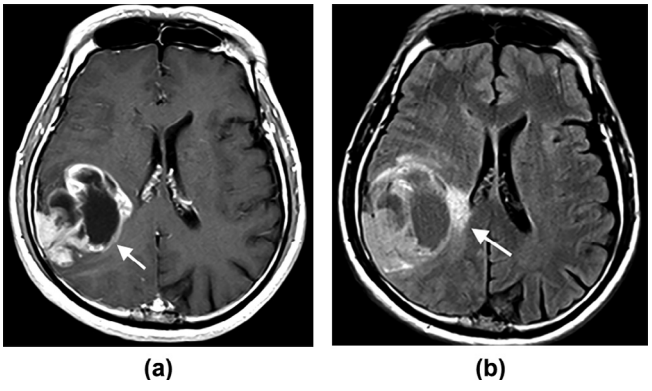

Fig. 1. IDH-wildtype GBM. (a) Post-contrast T1WI axial, (b) FLAIR axial. Post-contrast T1WI shows a heterogeneously enhancing mass in the right parietal lobe and a regular border (a). FLAIR shows hyperintensity around the mass as peritumoral edema (arrow) without hyperintensity, indicating low-grade glioma (b). FLAIR, fluid-attenuated inversion recovery; GBM, glioblastoma; IDH, isocitrate dehydrogenase; T1WI, T1-weighted imaging.

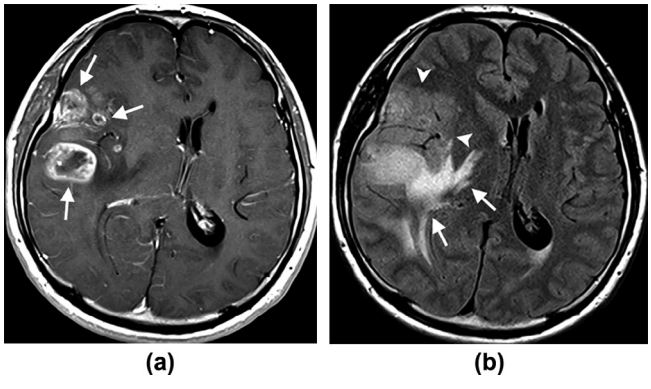

Fig. 2. IDH-wildtype GBM. (a) Post-contrast T1WI axial, (b) FLAIR axial. Postcontrast T1WI shows multiple heterogeneously enhancing masses in the right frontal and temporal lobe and a border that is partially irregular (a). FLAIR shows hyperintensity around the one of masses as peritumoral edema (arrow) and infiltrative hyperintensity with a mild signal lower than that for edema spreading further out from the edema as low-grade glioma (arrowhead) (b). It is estimated to be secondary GBM of IDH-wildtype. FLAIR, fluid-attenuated inversion recovery; GBM, glioblastoma; IDH, isocitrate dehydrogenase; T1WI, T1-weighted imaging.

Please cite this article as: T. Shimizu, S. Matsushima, N. Fukasawa et al., Differentiating between glioblastomas with and without isocitrate dehydrogenase gene mutation by findings on conventional magnetic resonance images, Journal of Clinical Neuroscience, https://doi.org/10.1016/j.jocn.2020.04.016

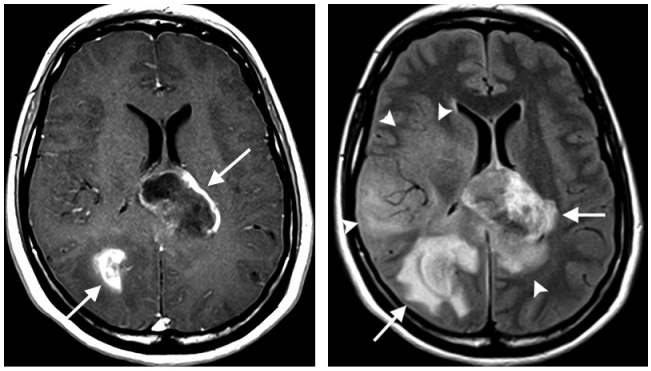

Fig. 3. IDH-mutant GBM. (a) Post-contrast T1WI axial, (b) FLAIR axial. Post-contrast T1WI shows a heterogeneously enhancing mass that extends from the left parietal lobe to the corpus callosum and a border that is partially irregular (a). A heterogeneously enhancing mass is also seen in the right parietal lobe (a). FLAIR shows hyperintensity around these masses as peritumoral edema (arrow) and infiltrative hyperintensity with a mild signal lower than for edema spreading further out from the edema as low-grade glioma (arrowhead) (b). FLAIR, fluid-attenuated inversion recovery; GBM, glioblastoma; IDH, isocitrate dehydrogenase; T1WI, T1-weighted imaging.

difficult to interpret, they are clinically important because they can be evaluated easily by conventional MRI. Previous reports indicate that gliosarcoma is often well-demarcated and presents superficially [8]; however, gliosarcoma is one of the subtypes of IDH-wildtype GBM and may simply reflect the characteristics of IDH-wildtype GBM.

In this study of GBM, we defined a background low-grade glioma as "an infiltrative T2 prolongation area without contrast enhancement and with mild lower signal than edema, spreading further out of T2 prolongation area including edema around the enhancing lesion" and checked for its presence or absence. De novo high-grade glioma has been reported to show early on as a non-specific small T2 prolongation area, which has been reported to increase in a short period of time and form a mass with contrast enhancement [9,10]. Therefore, it is unlikely that tumor components without contrast enhancement spread around the de novo GBM. If there is an infiltrative lesion that extends beyond the edema around a contrast-enhancing lesion, we consider it to be a low-grade glioma and a precursor to secondary GBM.

Given that most de novo GBMs are IDH-wildtype and many secondary GBMs are IDH-mutant, we considered that evaluation for the presence or absence of background low-grade glioma would be useful when assessing IDH gene mutation status; however, this was not the case in our study. Existence of IDH-mutant de novo GBM and IDH-wildtype secondary GBM was emphasized in a report published before the revised WHO classification [2], but in this study roughly one half of IDH-wildtype GBMs had a low-grade glioma in the background. Therefore, IDH-wildtype secondary GBM may be more frequent than previously reported; indeed, it may be more common overall than is recognized. In the WHO classification, de novo and secondary tumors are mainly categorized according to IDH gene mutation status; however, the situation may be more complicated in that genes other than those for IDH may be involved in the generation of secondary GBM. It is hoped that further molecular elucidation will be possible in the future. Moreover, in our study, low-grade glioma was observed in the background in 5 (83.3%) of 6 patients with a diagnosis of IDH-mutant GBM. Therefore, when a low-grade glioma cannot be confirmed, the GBM is more likely to be IDH-wildtype. In one patient with IDH-mutant GBM in whom a background low-grade glioma could not be confirmed, it is possible that the GBM component infiltrated more widely than the low-grade glioma component or that the low-grade glioma component was too small to be distinguished from the edema around the GBM.

This study has some limitations, including its retrospective design and the fact that the images were evaluated visually. Specifically, the presence or absence of low-grade glioma in the background could lead to a difference in judgment depending on the observer; however, it was difficult to quantitatively evaluate this parameter. Very good interobserver agreement was found between the two neuroradiologists who independently evaluated the images; however, quantitative evaluation would be a subject for another study. The other parameters were relatively easy to evaluate, and we believe that visual evaluation was not a problem. Another limitation is that the study population included patients who underwent repeat surgery and those who had undergone chemoradiotherapy before surgery. The possibility that preoperative treatment affected gene mutations and contrast enhancement cannot be ruled out; in particular, it seems likely that use of bevacizumab immediately before MRI affected the contrast enhancement. In this study, a patient in whom bevacizumab was used immediately before MRI was found to have IDH-mutant GBM and a low-grade glioma in the background on MRI. However, in this case, the background low-grade glioma component was confirmed histopathologically and was unlikely to have had a significant effect on the study results. It is difficult to determine if preoperative chemoradiotherapy affects IDH gene mutation status, and further investigation is necessary in the future. Furthermore, our study population was small. Nevertheless, our findings indicated a definite trend which will hopefully be confirmed in a future study that includes more cases. In the meantime, we consider that the results of this preliminary study are clinically significant and useful for predicting IDH gene mutations using conventional MRI.

5. Conclusion

There is a high likelihood that GBM is IDH-wildtype if it has a superficial location and shows regular border enhancement. Furthermore, when background low-grade glioma cannot be found on MRI, the possibility of IDH-wildtype GBM should be considered. Although most IDH-wildtype GBMs are considered to occur de novo, we found that approximately half of the cases had a low-grade glioma component in the background on MRI, so it may be

Table 2
Results for each imaging parameter evaluated.

	All patients (n = 23)	IDH-wildtype (n = 17)	IDH-mutant (n = 6)	p-value
Superficial location	13 (56.5%)	12 (70.6%)	1 (16.7%)	0.035
Irregular border (T2WI)	22 (95.7%)	16 (94.1%)	6 (100%)	0.739
Enhancing lesion with irregular border	11 (47.8%)	6 (35.3%)	5 (83.3%)	0.059
Multifocality	11 (47.8%)	8 (47.1%)	3 (50.0%)	0.634
Hemorrhage	20 (n = 21) (95.2%)	15 (n = 15) (100%)	5 (83.3%)	0.286
Low-grade glioma	14 (60.9%)	9 (52.9%)	5 (83.3%)	0.208

IDH, isocitrate dehydrogenase; T2WI, T2-weighted imaging.

Please cite this article as: T. Shimizu, S. Matsushima, N. Fukasawa et al., Differentiating between glioblastomas with and without isocitrate dehydrogenase gene mutation by findings on conventional magnetic resonance images, Journal of Clinical Neuroscience, https://doi.org/10.1016/j.jocn.2020.04.016

difficult to distinguish between de novo and secondary GBM using IDH gene mutation status.

Sources of support

This research did not receive any specific grant from funding agencies in the public, commercial, or not-for-profit sectors.

Declarations of interest

None.

References

[1] Louis DN, Perry A, Reifenberger G, von Deimling A, Figarella-Branger D, Cavenee WK, et al. The 2016 World Health Organization classification of tumors of the central nervous system: a summary. Acta Neuropathol 2016;131:803–20. https://doi.org/10.1007/s00401-016-1545-1.

[2] Nobusawa S, Watanabe T, Kleihues P, Ohgaki H. IDH1 mutations as molecular signature and predictive factor of secondary glioblastomas. Clin Cancer Res 2009;15:6002–7. https://doi.org/10.1158/1078-0432.CCR-09-0715.

[3] Carrillo JA, Lai A, Nghiemphu PL, Kim HJ, Phillips HS, Kharbanda S, et al. Relationship between tumor enhancement, edema, IDH1 mutational status, MGMT promoter methylation, and survival in glioblastoma. AJNR Am J Neuroradiol 2012;33:1349–55. https://doi.org/10.3174/ajnr.A2950.

[4] Lasocki A, Tsui A, Gaillard F, Tacey M, Drummond K, Stuckey S. Reliability of noncontrast-enhancing tumor as a biomarker of IDH1 mutation status in glioblastoma. J Clin Neurosci 2012;39:170–5. https://doi.org/10.1016/j.jocn.2017.01.007.

[5] Yamashita K, Hiwatashi A, Togao O, Kikuchi K, Hatae R, Yoshimoto K, et al. MR imaging-based analysis of glioblastoma multiforme: estimation of IDH1 mutation status. AJNR Am J Neuroradiol 2016;37:58–65. https://doi.org/10.3174/ajnr.A4491.

[6] Natsumeda M, Motohashi K, Igarashi H, Nozawa T, Abe H, Tsukamoto Y, et al. Reliable diagnosis of IDH-mutant glioblastoma by 2-hydroxyglutarate detection: a study by 3-T magnetic resonance spectroscopy. Neurosurg Rev 2018;41:641–7. https://doi.org/10.1007/s10143-017-0908-y.

[7] Chang P, Grinband J, Weinberg BD, Bardis M, Khy M, Cadena G, et al. Deep-learning convolutional neural networks accurately classify genetic mutations in gliomas. AJNR Am J Neuroradiol 2018;38:1201–7. https://doi.org/10.3174/ajnr.A5667.

[8] Zhang BY, Chen H, Geng DY, Yin B, Li YX, Zhong P, et al. Computed tomography and magnetic resonance features of gliosarcoma: a study of 54 cases. J Comput Assist Tomogr 2011;35:667–73. https://doi.org/10.1097/RCT.0b013e3182331128.

[9] Rossi R, Figus A, Corraine S. Early presentation of de novo high grade glioma with epileptic seizures: electroclinical and neuroimaging findings. Seizure 2010;19:470–4. https://doi.org/10.1016/j.seizure.2010.07.001.

[10] Ideguchi M, Kajiwara K, Goto H, Sugimoto K, Nomura S, Ikeda E, et al. MRI findings and pathological features in early-stage glioblastoma. J Neurooncol 2015;123:289–97. https://doi.org/10.1007/s11060-015-1797-y.

Please cite this article as: T. Shimizu, S. Matsushima, N. Fukasawa et al., Differentiating between glioblastomas with and without isocitrate dehydrogenase gene mutation by findings on conventional magnetic resonance images, Journal of Clinical Neuroscience, https://doi.org/10.1016/j.jocn.2020.04.016